Article

The Primate Cerebellum Selectively Encodes Unexpected Self-Motion

Jessica X. Brooks[1] and Kathleen E. Cullen[1,*]
[1]Department of Physiology, Aerospace Medical Research Unit, McGill University, Montréal, QC H3G 1Y6, Canada

Summary

Background: The ability to distinguish sensory signals that register unexpected events (exafference) from those generated by voluntary actions (reafference) during self-motion is essential for accurate perception and behavior. The cerebellum is most commonly considered in relation to its contributions to the fine tuning of motor commands and sensorimotor calibration required for motor learning. During unexpected motion, however, the sensory prediction errors that drive motor learning potentially provide a neural basis for the computation underlying the distinction between reafference and exafference.
Results: Recording from monkeys during voluntary and applied self-motion, we demonstrate that individual cerebellar output neurons encode an explicit and selective representation of unexpected self-motion by means of an elegant computation that cancels the reafferent sensory effects of self-generated movements. During voluntary self-motion, the sensory responses of neurons that robustly encode unexpected movement are canceled. Neurons with vestibular and proprioceptive responses to applied head and body movements are unresponsive when the same motion is self-generated. When sensory reafference and exafference are experienced simultaneously, individual neurons provide a precise estimate of the detailed time course of exafference.
Conclusions: These results provide an explicit solution to the longstanding problem of understanding mechanisms by which the brain anticipates the sensory consequences of our voluntary actions. Specifically, by revealing a striking computation of a sensory prediction error signal that effectively distinguishes between the sensory consequences of self-generated and externally produced actions, our findings overturn the conventional thinking that the sensory errors coded by the cerebellum principally contribute to the fine tuning of motor activity required for motor learning.

Introduction

The cerebellum has been proposed as a likely candidate site for a forward model that predicts the sensory consequences of self-generated action. Such a representation of the expected consequences of movement has emerged as an important theoretical concept in motor control (reviewed in [1, 2]). To date, this hypothesis has been chiefly considered in relation to the fine tuning of motor commands and sensorimotor calibration required for motor learning. In this context, the cerebellum computes a prediction of the sensory consequences of an action. This prediction is then compared to the sensory stimulation produced by the actual movement to compute an error signal that in turn guides the updating of the motor program. Indeed, there is evidence that sensory prediction errors drive motor learning [3, 4], and studies of neurologic patients [5, 6] and brain stimulation [7] suggest a role for cerebellum-dependent mechanisms.

However, sensory prediction errors arise not only as a result of changes in the motor apparatus and environment (i.e., conditions that drive motor learning) but also whenever we experience externally produced sensory stimuli. If externally imposed stimulation is systematically paired with voluntary movement, motor learning occurs [8]. In contrast, when sensory stimulation is unexpected, the computation of sensory prediction errors effectively enables the brain to distinguish between the consequences of our self-generated actions (sensory reafference) and stimulation that is externally produced (sensory exafference). Work in the vestibular system has provided evidence that indeed such a computation is performed. While afferents similarly encode vestibular reafference and exafference during self-motion [9, 10], neurons at the next stage of sensory processing preferentially respond to vestibular exafference [11, 12], indicating that the brain computes a cancellation signal required to suppress self-generated vestibular signals and thus selectively encode sensory exafference.

Despite long-standing interest in the computations required for accurate motor control, the neural mechanisms underlying the computation of sensory exafference remain unclear. It has been proposed that our brain constructs an internal model of the expected sensory consequences of movement based on an efference copy of the self-produced motor command [13–15]. Studies in the electrosensory system of fish have shown that their cerebellum-like circuitry computes predictions about the sensory consequences of the animals' own behavior [16]. However, while single-unit recording studies in primates [17] and imaging studies in normal subjects show increases in cerebellar activity when sensory feedback does not match what is expected [18, 19], the proposal that the cerebellum computes an explicit estimate of the sensory consequences of unexpected movement has not, to our knowledge, been tested. Moreover, because exafference and reafference are often experienced simultaneously, it is crucial to address whether neurons encode sensory prediction errors demonstrating the anticipation and cancellation of reafferent effects under conditions in which active and passive stimulation are concurrent.

Here, we recorded from individual neurons in the most medial of the deep cerebellar nuclei (rostral fastigial nucleus [rFN]), which constitutes a major output target of the cerebellar cortex [20] and sends strong projections to the vestibular nuclei, reticular formation, and spinal cord [20–23] to regulate postural control. We show for the first time that two separate processing streams within the cerebellum encode unexpected movements of the head (i.e., vestibular exafference) and body (i.e., combining vestibular and proprioceptive exafference)—even when applied concomitantly with voluntary motion. Our findings overturn the common assumption that the sensory errors coded by the cerebellum principally contribute to the fine tuning of motor activity required for motor learning by

*Correspondence: kathleen.cullen@mcgill.ca
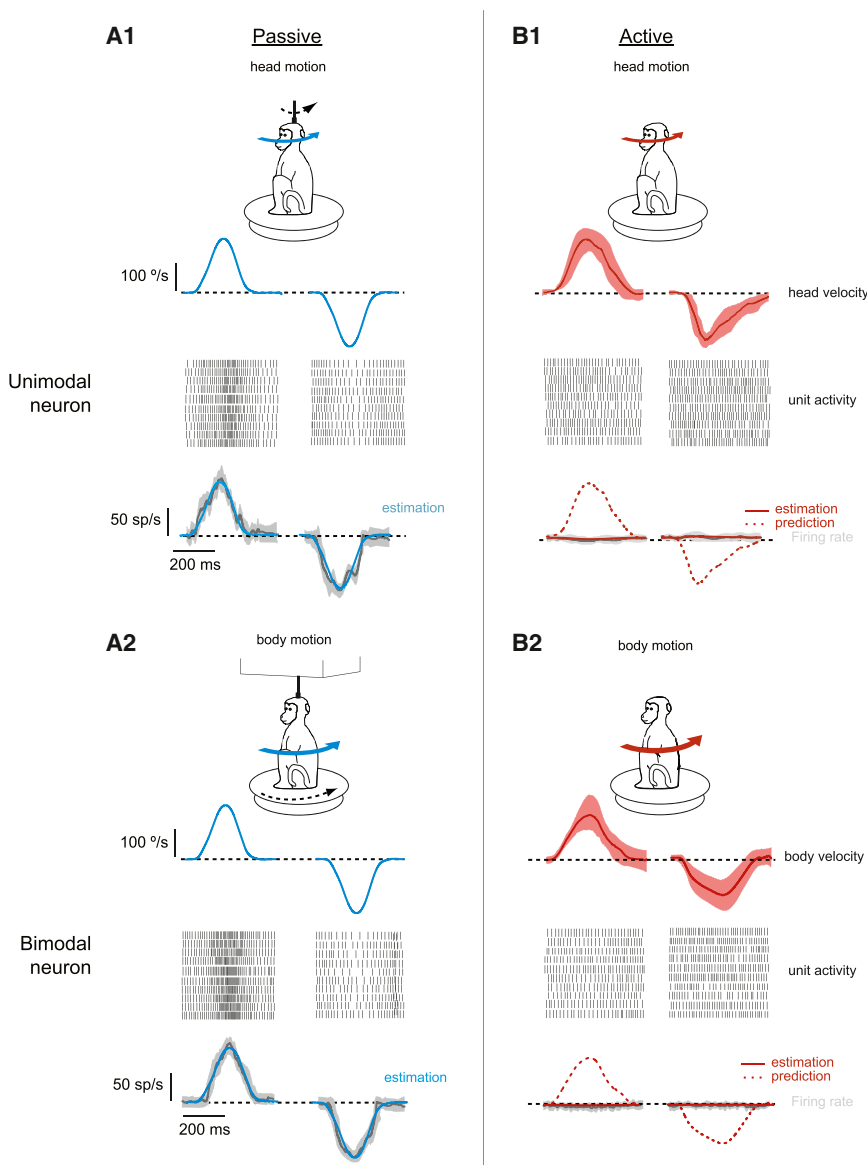
Figure 1. rFN Neuronal Responses Encode Unexpected, but Not Self-Produced, Sensory Inputs during Self-Motion

(A and B) Responses of example unimodal (A1 and B1) and bimodal (A2 and B2) neurons during passive (blue traces, A) and voluntary (red traces, B) motion paradigms. Top row: average head (unimodal neurons) and body (bimodal neurons) velocities for ten movements. The thickness of the shaded traces corresponds to the SD across trials. Raster plots illustrating the example neurons' responses for each trial are shown below. Bottom row: dark and lighter gray shading correspond to the average firing rates and SDs for the same ten movements. Overlaying blue (A1 and A2) and red (B1 and B2) lines show the estimated best fit to the firing rate based on a bias term and sensitivity to head (unimodal neurons) or body (bimodal neurons) motion. Note that both neurons showed robust modulation for passive motion (unimodal neuron, head velocity sensitivity: 0.41 [sp/s]/[°/s] and bimodal neuron, body velocity sensitivity: 0.36 [sp/s]/[°/s]), but responses were minimal when the same motion was self-produced (0.07 [sp/s]/[°/s] versus 0.05 [sp/s]/[°/s], respectively). Superimposed dashed red lines in the active condition (B1 and B2) show predicted responses based on each neuron's sensitivity to passive motion. Dashed black arrows on the cartoons show where the force was applied to generate passive motion. Raster plots were downsampled to improve visibility of the spikes. See also Figure S1.

rFN Neurons Encode Unexpected, but Not Self-Produced, Sensory Signals during Self-Motion

To date, prior investigations exclusively focused on understanding how these neurons, which constitute a major output target of the cerebellar cortex, encode sensory information under the passive (i.e., exafferent) stimulation conditions described above. However, in everyday life, vestibular and proprioceptive stimulation are the result of our own actions as well as motion resulting from external events. Accordingly, we performed a series of experiments to test the hypothesis that these neurons selectively encode unexpected, passively applied stimuli.

We first compared neuronal responses to passively applied and self-produced (i.e., active) stimuli with similar profiles. In the head-restrained condition, we applied vestibular and proprioceptive stimuli with a velocity profile designed to mimic that produced during active movement (i.e., "active-like" motion profiles; see Experimental Procedures and also Figures S1A1–S1A3 available online). The monkey's head was then released allowing the generation of actual active head and body movements. Figure 1 illustrates the striking difference in the responses of representative unimodal and bimodal neurons during passive (Figure 1A) versus active (Figure 1B) motion. The example cells were strongly modulated during passive head and body motion, respectively. However, when the monkey voluntarily produced motion that resulted in comparable sensory stimulation, the example neurons were virtually unresponsive to the same motion (87% and 86% response
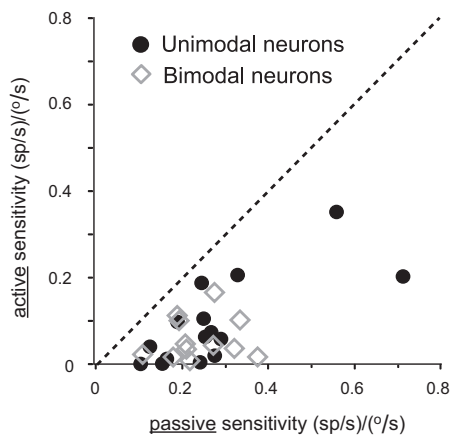
demonstrating the contribution of sensory prediction errors in the cerebellum to the computation of sensory exafference.

Results

All neurons included in the present report (n = 41) were sensitive to passive vestibular stimulation and were insensitive to eye movements, consistent with previous characterizations of rFN neurons [24–26]. Neurons were further characterized as either unimodal or bimodal, based on their sensitivity to applied stimulation of the neck proprioceptors. Notably, 52% of our sample (unimodal neurons; n = 21) were insensitive to proprioceptive stimulation. The other 48% (bimodal neurons; n = 20) were responsive to passive proprioceptive as well as vestibular stimulation. As a result of their vestibular sensitivity, unimodal neurons encode passive head motion, while bimodal neurons combine vestibular and neck proprioceptive inputs to encode passive body motion [24]. Thus, as expected, only the unimodal neurons responded during a third passive protocol in which the head was rotated on a stationary body.

Figure 2. Population Analysis: Cerebellar Neurons Preferentially Respond to Passive Stimulation

Scatterplot showing a cell-by-cell comparison of response sensitivities to active and passive motion for the populations of unimodal (black circles) and bimodal (gray diamonds) neurons. The dotted line represents unity. Mean neuronal sensitivities = 0.13 ± 0.03 versus 0.32 ± 0.05 (sp/s)/(°/s) for unimodal neurons and 0.11 ± 0.01 versus 0.31 ± 0.04 (sp/s)/(°/s) for bimodal neurons during active and passive motion, respectively. See also Figure S2.

attenuation, respectively). For completeness, analyses comparing responses to active versus passive motion were also carried out on unimodal neurons during body motion (Figure S1B1) and bimodal neurons during head motion (Figure S1B2), confirming that the expected lack of response remained in the active condition.

The observations shown in Figure 1 are summarized for the population in Figure 2. Neuronal responses in the active condition were not well predicted by sensitivities to vestibular and proprioceptive inputs in the passive condition. All data points fall well below the unity line, indicating that responses were suppressed during self-generated motion. Overall, for our entire population of neurons, modulation was reduced by ~70% when stimulation was self-produced (paired t test, p < 0.05 for both populations). This result suggests that rFN neurons do not provide a veridical representation of head (unimodal neurons) or body (bimodal neurons) motion during everyday activities, as their sensitivities to self-produced vestibular and proprioceptive input are attenuated.

The question thus arises: what accounts for the observed attenuation? During passive motion, rFN neuron responses can be predicted based on a linear summation of each neuron's sensitivity to vestibular and neck proprioceptor stimulation [24]. Accordingly, we tested whether this might also be the case during active motion. In contrast to the passive condition, neuronal responses could not be predicted based on a linear summation of their sensitivities to vestibular and proprioceptive stimulation (see Figure S2), indicating that an additional inhibitory signal is necessary to account for the attenuation observed in rFN neuron responses to self-generated sensory stimuli. Additionally, we tested the possibility that the production of a motor command alone can account for the attenuation of responses during active motion but found that this was not the case. Specifically, monkeys were unexpectedly restrained as they oriented to an eccentric target, where the intended but unrealized movement was demonstrated by the production of neck torque (Figures 3A1 and 3A2). The responses of unimodal and bimodal neuron

populations during attempted movements in either direction did not differ from resting rate (Figures 3B1 and 3B2; paired t test, p > 0.05 for both neuronal populations).

Neurons Selectively Respond to Passive Motion when Experienced Concurrently with Active Motion

Thus far, we have only considered active or passive stimulation in isolation; during daily activities, we commonly experience simultaneous active and passive motion. Thus the question remains: what information do rFN neurons encode when unexpected sensory signals are experienced concurrently with self-produced ones? We predicted that unimodal and bimodal neurons solve this problem by each selectively responding to passively applied stimulation, thereby providing representations of unexpected motion (i.e., passive head and body motion, respectively).

To test this proposal, we recorded neuronal activity as monkeys generated voluntary movements of their heads and bodies while simultaneously undergoing passive whole-body rotation. First, we considered unimodal neurons. If a given neuron selectively responded to passively applied vestibular stimulation, one would expect that during combined active-passive motion it should (1) remain unresponsive to any actively generated motion of the head relative to space but (2) continue to robustly encode head motion due to the passively applied rotation. Figure 4 illustrates the response of an example unimodal neuron during passive whole-body rotation alone (Figure 4A) and combined with simultaneous active head (Figures 4B and 4C, open boxes) and body (Figure 4C, shaded box) movements. Comparison across panels reveals that the neuron selectively encoded only the passive component of motion (passive head-motion-only prediction, blue trace) rather than absolute head-in-space motion (total head-motion prediction, black trace). Thus, consistent with our prediction, our example unimodal neuron faithfully encoded passively applied vestibular stimulation regardless of whether it occurred in isolation or simultaneously with self-generated vestibular stimulation.

Using the same approach, we next tested bimodal neurons. In this case, if a given neuron selectively responded to passively applied vestibular and proprioceptive stimulation, one would expect that during combined active and passive motion it should (1) remain unresponsive to active body motion relative to space but (2) robustly encode body motion due to the passively applied rotation. Figure 5 illustrates the response of an example bimodal neuron during passive whole-body rotation alone (Figure 5A) and combined with active body (Figure 5B, shaded box) and head (Figures 5B and 5C, open boxes) movements. Comparison across panels reveals that the neuron selectively encoded only the passive component of the motion (passive body-motion-only prediction, blue trace), rather than absolute body-in-space motion (total body-motion prediction, dashed black trace). Furthermore, this neuron's response was also not altered by concurrent active head movements (Figures 5B and 5C, open boxes). Thus, in agreement with our prediction, our example bimodal neuron faithfully encoded passively applied vestibular and proprioceptive stimulation regardless of whether it occurred in isolation or simultaneously with self-generated stimulation.

What Signal Do Cerebellar Neurons Encode during Self-Motion?

Cerebellar-dependent mechanisms are thought to play a central role in computing sensory prediction errors—a signal that
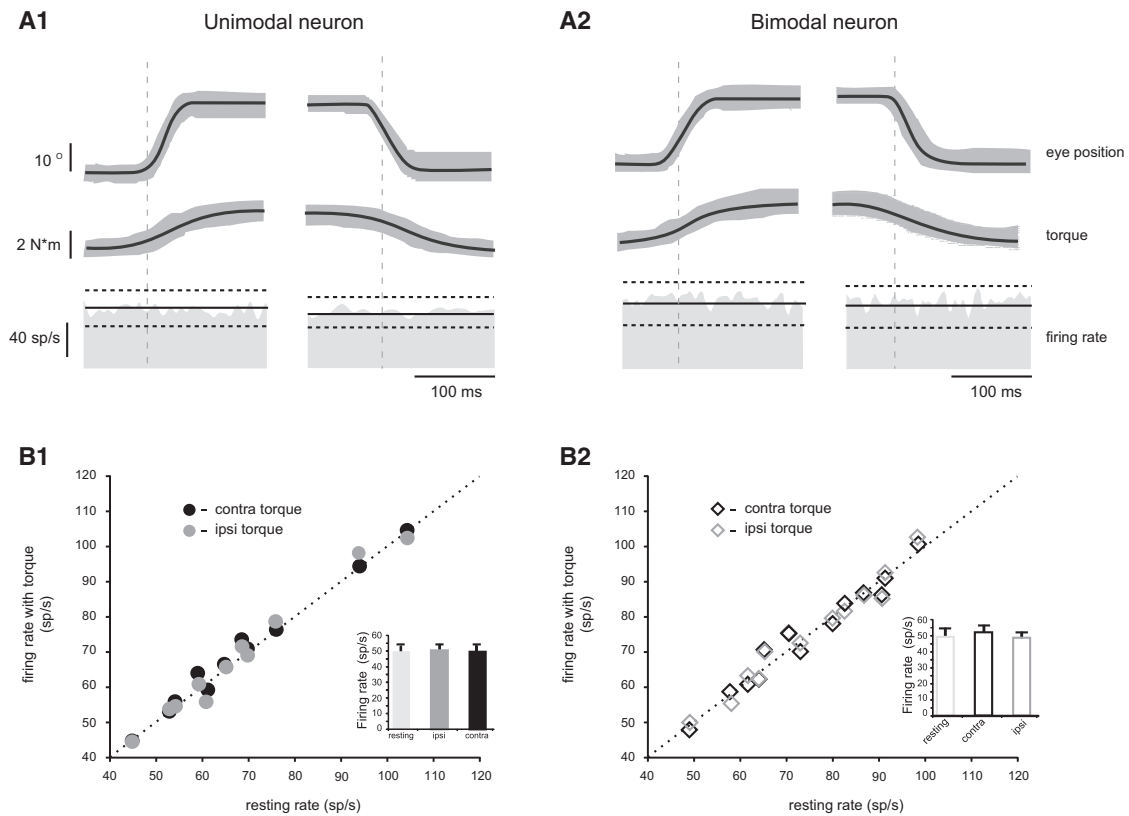
Figure 3. The Production of Motor Commands Does Not Account for Neuronal Response Attenuation

(A1 and A2) The example unimodal (A1) and bimodal (A2) neurons did not display any related modulation for torques produced either in the ipsilateral (i.e., "ipsi"; left) or contralateral (i.e., "contra"; right) directions. Traces are aligned on torque onset and show eye position, torque, and firing rates (bottom trace) averaged (±SD) over ten movements in each direction.

(B1 and B2) Population analysis: mean firing rates of unimodal (B1) and bimodal (B2) neurons for periods of ipsilaterally and contralaterally directed torque plotted as a function of resting rate. The slope of the regression line was not different from 1 (p > 0.05), indicating that torque production did not influence neuronal activity. Insets: mean response rates of both neuron populations do not differ across conditions (paired t test; p > 0.05 for both neuronal populations).

would represent the sensory consequences of unexpected sensory stimulation (i.e., exafference) during self-generated actions. Given that the rFN receives direct input from the output cells of the cerebellar cortex (i.e., Purkinje cells), we hypothesized that rFN neurons would explicitly encode exafference. To directly test this hypothesis, we next compared the sensitivities of each unimodal and bimodal neuron in our population during combined active and passive motion of the head (Figure 4) or body (Figure 5), respectively, to their sensitivity to the same motion passively applied in isolation. If a given neuron explicitly encodes exafference, then its sensitivity to sensory stimulation resulting from the passive component of motion should be the same, regardless of whether it occurred concurrently with active motion or was applied in isolation. Additionally, its sensitivity to sensory stimulation resulting from the active component of motion should be markedly reduced relative to its passive sensitivity.

Figure 6 shows a comparison of each neuron's sensitivity to the passive (Figure 6A) and active (Figure 6B) components of motion to the same neuron's sensitivity to passive motion applied alone. Consistent with the first part of our hypothesis, unimodal and bimodal neurons responded similarly to passive motion in both conditions (Figure 6A); the slopes of the regression lines were not different from unity (p = 0.63 and 0.95, respectively). Thus, rFN neurons faithfully encoded

exafference during passive motion, whether it occurred concurrently with active movements or in isolation. Figure 6B shows that, consistent with the second part of our hypothesis, the responses of unimodal and bimodal neurons were significantly (p < 0.05) attenuated during active as compared to passive motion (68% and 71% attenuation, respectively). All points fell below the unity line, clearly demonstrating that rFN neurons remain unresponsive to sensory stimulation that is the result of active motion, even when it occurs concurrently with passively applied motion. Taken together, our results not only demonstrate for the first time that unimodal and bimodal neurons differentiate between the sensory consequences of active and passive motion but also show that this facilitates the selective and explicit encoding of the passive components of head and body motion, respectively. Thus, our findings are consistent with the proposal that the responses of individual rFN neurons reveal the output of a computation providing an explicit estimate of the detailed time course of exafference (e.g, blue traces in Figures 4 and 5).

Discussion

To date, all previous single-unit recording studies in the vestibular cerebellum have exclusively focused on understanding how passively applied stimuli are encoded during motion
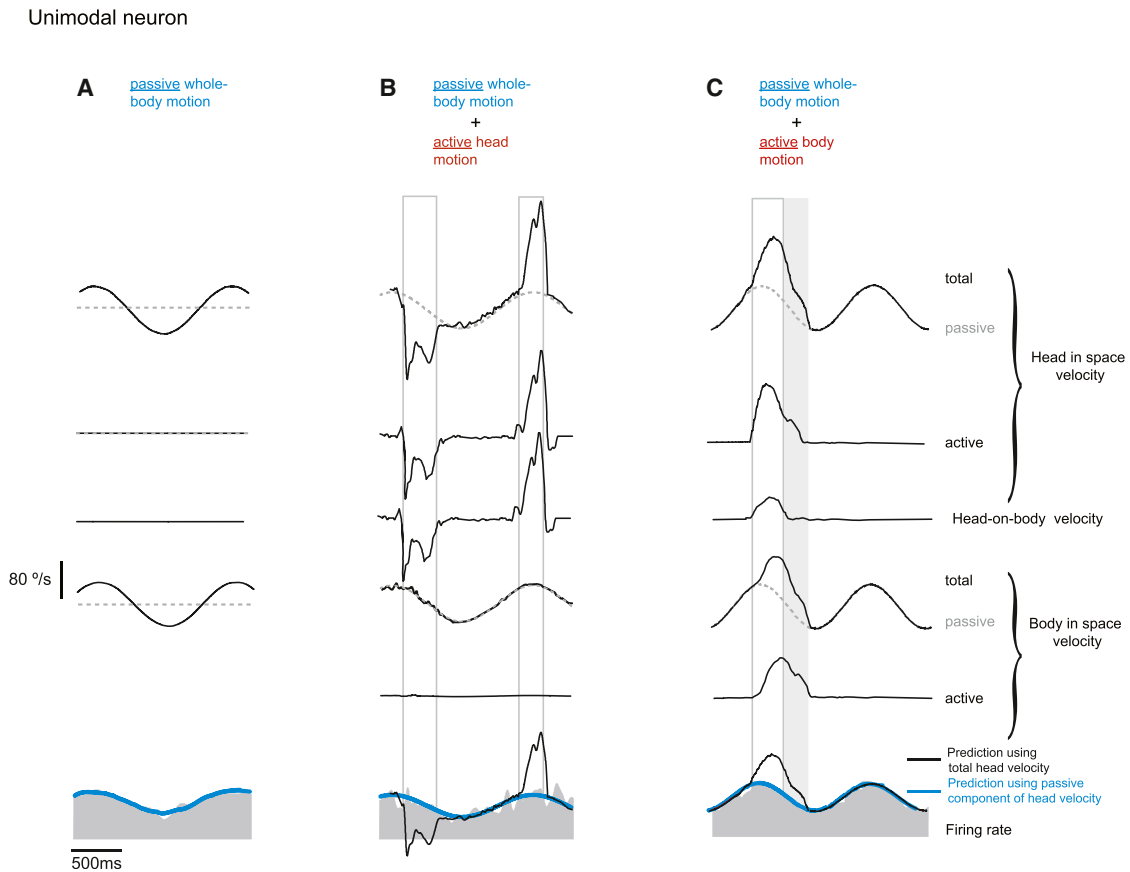
Figure 4. Unimodal Neurons Selectively Respond to Passive Head Motion when Experienced Concurrently with Active Motion

(A) Activity of an example unimodal neuron during passive sinusoidal whole-body rotation applied alone.

(B and C) Response of the same unimodal neuron during a paradigm where the monkey generated voluntary head (B) or body (C) movements while being simultaneously passively rotated. Superimposed on the firing rates are predictions based on passive head motion only (blue traces) and total head motion (black traces).

(reviewed in [27, 28]). However, during daily activities, we commonly experience simultaneous active and passive motion. Our data clearly show that two separate processing streams within rhesus macaque cerebellum selectively encode sensory information arising from externally applied motion. Specifically, unimodal neurons selectively respond to vestibular exafference to encode unexpected head-in-space velocity, while bimodal neurons respond to both vestibular and proprioceptive exafference to encode unexpected body-in-space velocity. Thus, taken together, our findings reveal for the first time the output of an elegant computation in which two distinct neuron populations selectively and dynamically encode unexpected head versus body motion relative to space.

Theoretically, the computation of exafference requires a comparison between an internal estimate of the sensory consequences of self-generated action (i.e., forward model) and the actual sensory feedback [14, 29]. There is accumulating evidence that this comparison is made, at least in part, at the level of the cerebellar cortex. Notably, complex and simple spike responses decrease and increase, respectively, during active versus passive wrist movements [17], consistent with the idea that reafferent sensory feedback is suppressed. Additionally, the results of human imaging studies are consistent with the proposal that cerebellar cortex is involved in the suppression of tactile reafference during a

self-produced "tickle" [30] and in signaling of the discrepancy between predicted and actual sensory feedback when subjects encounter unexpected load changes in a voluntary lifting task [19].

The ability to control posture and estimate self-motion depends strongly on the integration of vestibular and proprioceptive information [31–34] and is profoundly disrupted in cerebellar patients [35]. The rFN is ideally situated anatomically to contribute to postural control, as it receives descending projections from the anterior vermis of the cerebellum [20] as well as ascending neck proprioceptive input via the central cervical nucleus and the external cuneate nucleus [36], and it in turn projects to vestibular neurons, reticular formation, and spinal cord [20–23]. Accordingly, our data (Figures 4 and 5) can account for how the brain selectively responds to adjust postural tone in response to unexpected motion experienced during voluntary motion. Notably, our findings also provide significant insight into the neural mechanisms underlying the suppression of sensory reafference in vestibular and proprioceptive processing. In primates, vestibular afferents do not make the distinction between active and passive motion (e.g., [9, 10]). Similarly, proprioceptive and somatosensory inputs are largely intact during active motion at the level of the periphery and spinal cord [37, 38]. Reafferent signals are, however, suppressed at subsequent stages of processing. For example, reafferent vestibular input is suppressed at the
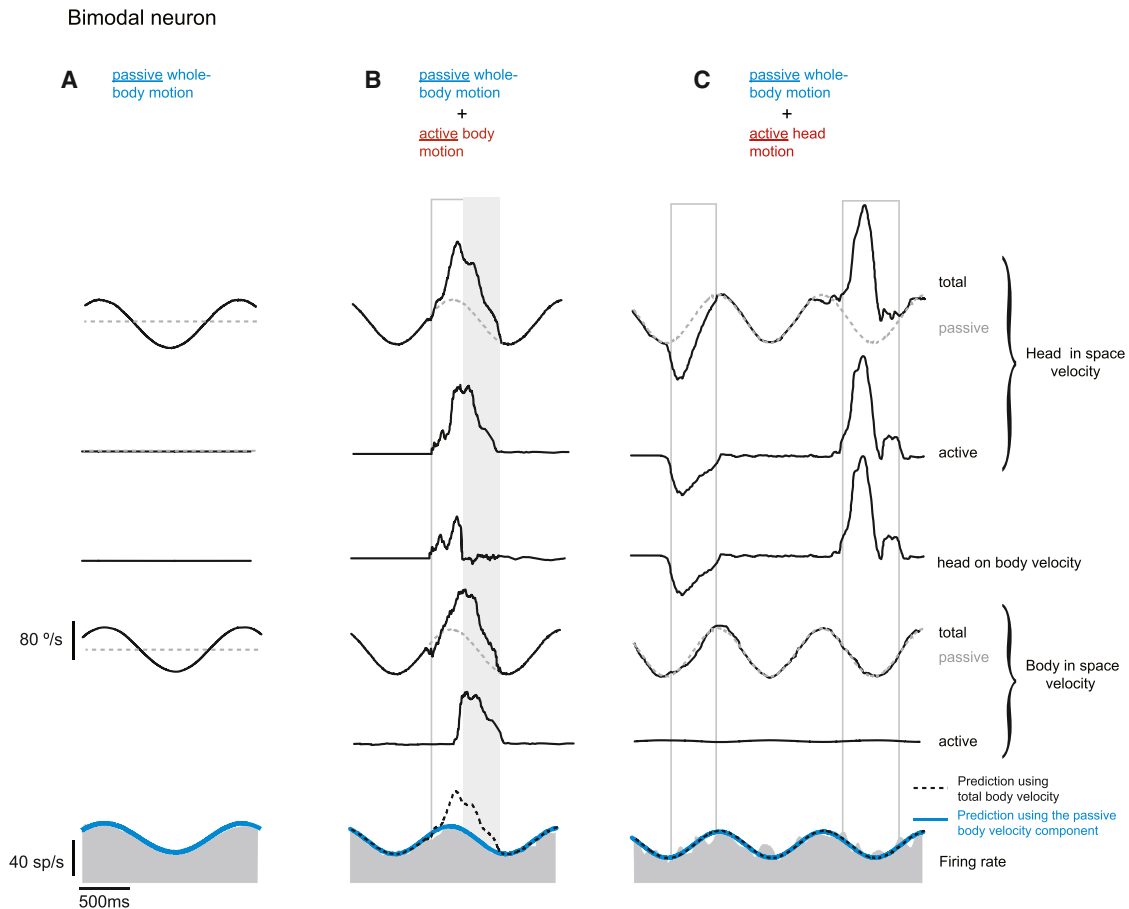
Bimodal neuron

Figure 5. Bimodal Neurons Selectively Respond to Passive Body Motion when Experienced Concurrently with Active Motion

(A) Activity of an example bimodal neuron during passive sinusoidal whole-body rotation applied alone.

(B and C) Response of the same bimodal neuron during a paradigm where the monkey generated voluntary body (B) or head (C) movements while being simultaneously passively rotated. Superimposed on the firing rates are predictions based on passive body motion only (blue traces) and total body motion (dashed black traces).

first central stage of vestibular processing (i.e., neurons in the vestibular nuclei). Prior to this study, the source of the suppression signal required to suppress vestibular afferent input at this first stage of sensory processing was unknown [11, 12]. The rFN sends a strong and direct projection to the vestibular nuclei [20–23], and thus we speculate, based on our current results, that the unimodal neurons of the rFN contribute to the selective processing of exafference in early vestibular processing.

Ultimately, further studies in the cerebellar cortex and deep nuclei are required to provide a deeper understanding of the mechanism underlying the suppression of sensory reafference. An interesting parallel can be found in the electrosensory system of fish, in which the cerebellum-like circuitry computes a negative image of the predicted sensory consequences of the animals' own behavior to suppress reafference [39, 40]. Interestingly, however, our results show that the rules that govern the cancellation of self-generated vestibular signals in the primate cerebellum differ from those in the fish electrosensory system. In the latter case, a cancellation signal is produced to eliminate self-generated inputs regardless of whether or not the fish's motor command to elicit an electric organ discharge is actually executed. In contrast, reafference cancellation in the primate cerebellum

appears to be characterized by a more sophisticated computation, in which the differences between expected and actual sensory inputs are used to selectively modulate sensory processing of self-motion, as when motor output is blocked, there is no negative image evident in the firing of rFN neurons (Figure 3).

The cerebellum is most commonly considered in relation to its contributions to the fine tuning of motor commands and the sensorimotor calibration required for motor learning. In this context, there is considerable debate whether cerebellar activity is consistent with an inverse or forward model (reviewed in [41]). Support for the latter view is provided by recent evidence that cerebellar Purkinje cell responses encode the predicted consequence of movement rather than actual movement [42, 43]. The difference between this prediction of the forward model and actual sensory feedback is proposed to drive motor learning. In the current study, we found that neurons in the cerebellar deep nuclei reveal the output of such a computation, namely an explicit estimate of the detailed time course of unexpected sensory input (i.e., sensory prediction error). Notably, however, this signal was encoded in conditions that did not require motor learning. Thus, our results support the view that the output of the cerebellum is consistent with a forward model, and they further
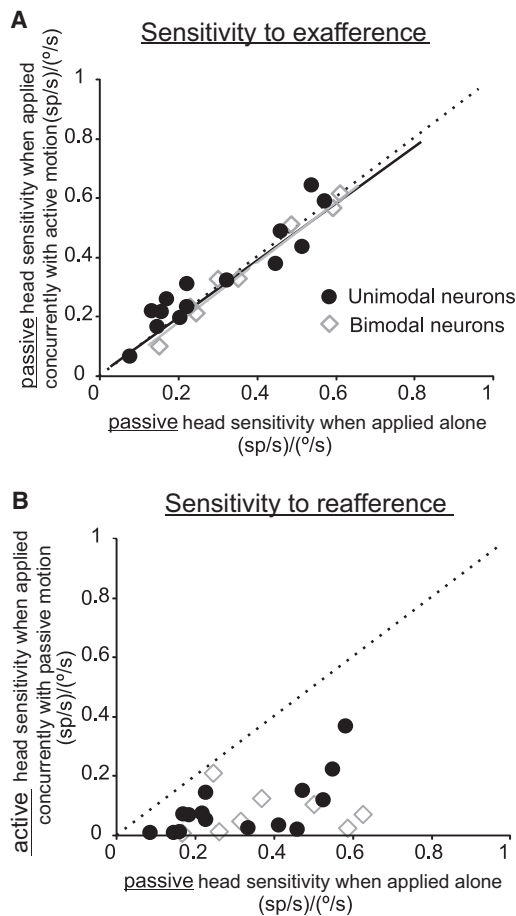
A Sensitivity to exafference

B Sensitivity to reafference

Figure 6. rFN Neurons Encode an Explicit Estimate of Exafference

(A) Scatterplot of unimodal (black circles) and bimodal (open diamonds) neuron sensitivities to the passive component of simultaneously occurring active and passive rotation versus neuronal sensitivities to passive rotations occurring alone. The sensitivity of rFN neurons to passive motion was the same whether it occurred in isolation or in combination with active movements (slope = 0.91, p = 0.67 and slope = 0.99, p = 0.95 for unimodal and bimodal neurons, respectively).

(B) Scatterplot of unimodal (black circles) and bimodal (open diamonds) neuron sensitivities to the active component of simultaneously active and passive rotation versus sensitivities to passive rotations occurring alone. Comparison with (A) indicates that neuronal responses to active motion were significantly selectively suppressed in this condition.

suggest that this computation underlies the brain's ability to distinguish between expected and unexpected sensory inputs.

Experimental Procedures

Surgical Procedures and Data Acquisition

All experimental protocols were approved by the McGill University Animal Care Committee and were in compliance with the Canadian Council on Animal Care guidelines. Two rhesus monkeys (*Macaca mulatta*) were prepared for extracellular recording using aseptic surgical techniques as previously described by Brooks and Cullen [24].

During experiments, monkeys trained to follow a target light sat in a primate chair attached to a vestibular turntable. Single-unit activity was recorded using enamel-insulated tungsten microelectrodes, and gaze, head, and body positions were measured using the search-coil technique [44, 45]. Target position and motor velocity were controlled online [46] and recorded on digital audio tape for later playback with concurrent gaze, head position, body position, and unit activity. During playback,

action potentials were discriminated (BAK Electronics), and recorded position and table velocity signals were low-pass filtered at 250 Hz (eight-pole antialiasing Bessel filter) and sampled at 1 kHz.

Head-Restrained Paradigms

Passive vestibular (i.e., whole-body rotation) and proprioceptive (body-under-head rotation) stimuli were first applied as described by Brooks and Cullen [24]. Stimuli included (1) 1 Hz sinusoidal (±40°/s) and (2) "active-like motion" trajectories corresponding to those produced during active head-unrestrained gaze shifts (see "head-free paradigms" below). Units were classified as bimodal if they responded to proprioceptive stimulation (sensitivity > 0.1 [sp/s]/[°/s]) and as unimodal if insensitive.

To quantify the integration of vestibular and proprioceptive inputs, we next characterized neuronal responses during head-on-body rotations. A torque motor (Kollmorgen) attached to the monkey's head delivered sinusoidal and active-like stimuli. Note that sensitivities to sinusoidal [24] and active-like motion (Figures S1A–S3) were not statistically different during passive whole-body, body-under-head, and head-on-body rotation paradigms (p > 0.05 for both neuron types during these three paradigms).

Finally, neuronal responses were recorded while each monkey attempted to orient to a target with its head and body restrained. The large torques measured during this paradigm (>1 Nm) verified that monkeys generated motor commands that were unrealized due to the restraint.

Head-Free Paradigms

After a neuron was fully characterized in the head-restrained condition, the monkey's head was carefully released to maintain neuronal isolation. Once released, the monkey was able to rotate its head freely in the yaw axis. The same neuron was then recorded while monkeys made voluntary (1) eye-head movements (necessitating neck muscle activation) with the body stationary and (2) eye-head-body movements (necessitating both neck and axial muscle activation). Additionally, to allow the characterization of response to simultaneous voluntary and passive movements, head- and body-unrestrained monkeys were passively rotated (1 Hz, ±40°/s peak velocity).

Analysis of Neuronal Discharges

Data were imported into the MATLAB (MathWorks) programming environment for analysis, filtering, and processing, as previously described [14]. Neural firing rate was represented using a spike density function in which a Gaussian function was convolved with the spike train (SD of 5 ms) [47].

We first verified that each neuron neither paused nor burst during saccades and was unresponsive to changes in eye position during fixation [11, 48]. A least-squares regression analysis was then used to describe each unit's response to whole-body and body-under-head rotations:

$$\hat{fr}(t) = b + c_{v,i}\,\dot{X}_i(t) + c_{a,i}\,\ddot{X}_i(t) \qquad \text{(Equation 1)}$$

where $\hat{fr}$ is the estimated firing rate, b is a bias term, $C_{v,i}$ and $C_{a,i}$ are coefficients representing velocity and acceleration sensitivities respectively to head (*i* = 1) or body motion (*i* = 2), and $\dot{X}_i$ and $\ddot{X}_i$ are head (*i* = 1) velocity and acceleration and body (*i* = 2) velocity and acceleration (during whole-body and body-under-head rotations), respectively.

A similar approach was used to estimate sensitivities to passive and active head-on-body movements. In these conditions, neck proprioceptive and vestibular sensitivities cannot be dissociated and are estimated as a single coefficient. Estimated sensitivities were compared to those predicted from linear summation of the vestibular and proprioceptive sensitivities estimated for the same neuron during passive whole-body and body-under-head rotations (termed linear model), respectively. During active body movements, where the head and body moved together in space, the data was fit with estimated vestibular coefficients (Equation 1).

To quantify the ability of the linear regression analysis to model neuronal discharges, we determined the variance accounted for (VAF) in each regression equation as previously described [14]. Values are expressed as mean ± SEM, and Student's t tests were used to assess differences between conditions.

Supplemental Information

Supplemental Information includes two figures and can be found with this article online at http://dx.doi.org/10.1016/j.cub.2013.04.029.

References

1. Wolpert, D.M., Miall, R.C., and Kawato, M. (1998). Internal models in the cerebellum. Trends Cogn. Sci. *2*, 338–347.
2. Krakauer, J.W., and Mazzoni, P. (2011). Human sensorimotor learning: adaptation, skill, and beyond. Curr. Opin. Neurobiol. *21*, 636–644.
3. Mazzoni, P., and Krakauer, J.W. (2006). An implicit plan overrides an explicit strategy during visuomotor adaptation. J. Neurosci. *26*, 3642–3645.
4. Wong, A.L., and Shelhamer, M. (2011). Exploring the fundamental dynamics of error-based motor learning using a stationary predictive-saccade task. PLoS ONE *6*, e25225.
5. Taylor, J.A., Klemfuss, N.M., and Ivry, R.B. (2010). An explicit strategy prevails when the cerebellum fails to compute movement errors. Cerebellum *9*, 580–586.
6. Tseng, Y.W., Diedrichsen, J., Krakauer, J.W., Shadmehr, R., and Bastian, A.J. (2007). Sensory prediction errors drive cerebellum-dependent adaptation of reaching. J. Neurophysiol. *98*, 54–62.
7. Galea, J.M., Vazquez, A., Pasricha, N., de Xivry, J.J., and Celnik, P. (2011). Dissociating the roles of the cerebellum and motor cortex during adaptive learning: the motor cortex retains what the cerebellum learns. Cereb. Cortex *21*, 1761–1770.
8. Davidson, P.R., and Wolpert, D.M. (2003). Motor learning and prediction in a variable environment. Curr. Opin. Neurobiol. *13*, 232–237.
9. Cullen, K.E., and Minor, L.B. (2002). Semicircular canal afferents similarly encode active and passive head-on-body rotations: implications for the role of vestibular efference. J. Neurosci. *22*, RC226.
10. Jamali, M., Sadeghi, S.G., and Cullen, K.E. (2009). Response of vestibular nerve afferents innervating utricle and saccule during passive and active translations. J. Neurophysiol. *101*, 141–149.
11. Roy, J.E., and Cullen, K.E. (2001). Selective processing of vestibular reafference during self-generated head motion. J. Neurosci. *21*, 2131–2142.
12. Roy, J.E., and Cullen, K.E. (2004). Dissociating self-generated from passively applied head motion: neural mechanisms in the vestibular nuclei. J. Neurosci. *24*, 2102–2111.
13. Sperry, R.W. (1950). Neural basis of the spontaneous optokinetic response produced by visual inversion. J. Comp. Physiol. Psychol. *43*, 482–489.
14. von Holst, E., and Mittelstaedt, H. (1950). Das reafferenzprinzip. Naturwissenschaften *37*, 464–476.
15. Jeannerod, M., Kennedy, H., and Magnin, M. (1979). Corollary discharge: its possible implications in visual and oculomotor interactions. Neuropsychologia *17*, 241–258.
16. Sawtell, N.B., and Bell, C.C. (2008). Adaptive processing in electrosensory systems: links to cerebellar plasticity and learning. J. Physiol. Paris *102*, 223–232.
17. Bauswein, E., Kolb, F.P., Leimbeck, B., and Rubia, F.J. (1983). Simple and complex spike activity of cerebellar Purkinje cells during active and passive movements in the awake monkey. J. Physiol. *339*, 379–394.
18. Blakemore, S.J., Frith, C.D., and Wolpert, D.M. (1999). Spatio-temporal prediction modulates the perception of self-produced stimuli. J. Cogn. Neurosci. *11*, 551–559.
19. Jenmalm, P., Schmitz, C., Forssberg, H., and Ehrsson, H.H. (2006). Lighter or heavier than predicted: neural correlates of corrective mechanisms during erroneously programmed lifts. J. Neurosci. *26*, 9015–9021.
20. Batton, R.R., 3rd, Jayaraman, A., Ruggiero, D., and Carpenter, M.B. (1977). Fastigial efferent projections in the monkey: an autoradiographic study. J. Comp. Neurol. *174*, 281–305.
21. Homma, Y., Nonaka, S., Matsuyama, K., and Mori, S. (1995). Fastigiofugal projection to the brainstem nuclei in the cat: an anterograde PHA-L tracing study. Neurosci. Res. *23*, 89–102.
22. Carleton, S.C., and Carpenter, M.B. (1983). Afferent and efferent connections of the medial, inferior and lateral vestibular nuclei in the cat and monkey. Brain Res. *278*, 29–51.
23. Shimazu, H., and Smith, C.M. (1971). Cerebellar and labyrinthine influences on single vestibular neurons identified by natural stimuli. J. Neurophysiol. *34*, 493–508.
24. Brooks, J.X., and Cullen, K.E. (2009). Multimodal integration in rostral fastigial nucleus provides an estimate of body movement. J. Neurosci. *29*, 10499–10511.
25. Shaikh, A.G., Meng, H., and Angelaki, D.E. (2004). Multiple reference frames for motion in the primate cerebellum. J. Neurosci. *24*, 4491–4497.
26. Gardner, E.P., and Fuchs, A.F. (1975). Single-unit responses to natural vestibular stimuli and eye movements in deep cerebellar nuclei of the alert rhesus monkey. J. Neurophysiol. *38*, 627–649.
27. Angelaki, D.E., Yakusheva, T.A., Green, A.M., Dickman, J.D., and Blazquez, P.M. (2010). Computation of egomotion in the macaque cerebellar vermis. Cerebellum *9*, 174–182.
28. Barmack, N.H., and Yakhnitsa, V. (2011). Topsy turvy: functions of climbing and mossy fibers in the vestibulo-cerebellum. Neuroscientist *17*, 221–236.
29. Miall, R.C., Weir, D.J., Wolpert, D.M., and Stein, J.F. (1993). Is the cerebellum a smith predictor? J. Mot. Behav. *25*, 203–216.
30. Blakemore, S.J., Wolpert, D.M., and Frith, C.D. (1999). The cerebellum contributes to somatosensory cortical activity during self-produced tactile stimulation. Neuroimage *10*, 448–459.
31. Mergner, T., Anastasopoulos, D., Becker, W., and Deecke, L. (1981). Discrimination between trunk and head rotation; a study comparing neuronal data from the cat with human psychophysics. Acta Psychol. (Amst.) *48*, 291–301.
32. Mergner, T., Nardi, G.L., Becker, W., and Deecke, L. (1983). The role of canal-neck interaction for the perception of horizontal trunk and head rotation. Exp. Brain Res. *49*, 198–208.
33. Mergner, T., Siebold, C., Schweigart, G., and Becker, W. (1991). Human perception of horizontal trunk and head rotation in space during vestibular and neck stimulation. Exp. Brain Res. *85*, 389–404.
34. Horak, F.B., Shupert, C.L., Dietz, V., and Horstmann, G. (1994). Vestibular and somatosensory contributions to responses to head and body displacements in stance. Exp. Brain Res. *100*, 93–106.
35. Kammermeier, S., Kleine, J., and Büttner, U. (2009). Vestibular-neck interaction in cerebellar patients. Ann. N Y Acad. Sci. *1164*, 394–399.
36. Voogd, J., Gerrits, N.M., and Ruigrok, T.J. (1996). Organization of the vestibulocerebellum. Ann. N Y Acad. Sci. *781*, 553–579.
37. Jones, K.E., Wessberg, J., and Vallbo, A.B. (2001). Directional tuning of human forearm muscle afferents during voluntary wrist movements. J. Physiol. *536*, 635–647.
38. Seki, K., and Fetz, E.E. (2012). Gating of sensory input at spinal and cortical levels during preparation and execution of voluntary movement. J. Neurosci. *32*, 890–902.
39. Bell, C.C., Han, V., and Sawtell, N.B. (2008). Cerebellum-like structures and their implications for cerebellar function. Annu. Rev. Neurosci. *31*, 1–24.
40. Requarth, T., and Sawtell, N.B. (2011). Neural mechanisms for filtering self-generated sensory signals in cerebellum-like circuits. Curr. Opin. Neurobiol. *21*, 602–608.
41. Medina, J.F. (2011). The multiple roles of Purkinje cells in sensori-motor calibration: to predict, teach and command. Curr. Opin. Neurobiol. *21*, 616–622.
42. Pasalar, S., Roitman, A.V., Durfee, W.K., and Ebner, T.J. (2006). Force field effects on cerebellar Purkinje cell discharge with implications for internal models. Nat. Neurosci. *9*, 1404–1411.
43. Hewitt, A.L., Popa, L.S., Pasalar, S., Hendrix, C.M., and Ebner, T.J. (2011). Representation of limb kinematics in Purkinje cell simple spike discharge is conserved across multiple tasks. J. Neurophysiol. *106*, 2232–2247.
44. Fuchs, A.F., and Robinson, D.A. (1966). A method for measuring horizontal and vertical eye movement chronically in the monkey. J. Appl. Physiol. *21*, 1068–1070.
45. Judge, S.J., Richmond, B.J., and Chu, F.C. (1980). Implantation of magnetic search coils for measurement of eye position: an improved method. Vision Res. *20*, 535–538.

46. Hayes, A.V., Richmond, B.J., and Optican, L.M. (1982). A UNIX-based multiple process system for real-time data acquisition and control. Western Electronic Show and Conference Proceedings *2*, 1–10.

47. Cullen, K.E., Rey, C.G., Guitton, D., and Galiana, H.L. (1996). The use of system identification techniques in the analysis of oculomotor burst neuron spike train dynamics. J. Comput. Neurosci. *3*, 347–368.

48. Roy, J.E., and Cullen, K.E. (1998). A neural correlate for vestibulo-ocular reflex suppression during voluntary eye-head gaze shifts. Nat. Neurosci. *1*, 404–410.